Alkylidyne-alkyne coupling on triruthenium clusters. Isomerization of (.mu.-H)Ru3(.mu.3-.eta.3-EtSCCRCR)(CO)9 (R = Me or Ph) to Ru3(.mu.-SEt)(CO)9(.mu.3-.eta.3-CCRCHR), an intermediate in alkylidyne chain growth. The crystal structure of Ru3(.mu.-SEt)(.mu.3-.eta.3-CCPhCHPh)(CO)9

Joseph W. Ziller, David K. Bower, Dennis M. Dalton, Jerome B. Keister, and Melvyn Rowen. Churchill

Organometallics, **1989**, 8 (2), 492-497• DOI: 10.1021/om00104a034 • Publication Date (Web): 01 May 2002

Alkylidyne–Alkyne Coupling on Triruthenium Clusters. Isomerization of $(\mu\text{-H})Ru_3(\mu_3\text{-}\eta^3\text{-EtSCCRCR})(CO)_9$ (R = Me or Ph) to $Ru_3(\mu\text{-SEt})(CO)_9(\mu_3\text{-}\eta^3\text{-CCRCHR})$, an Intermediate in Alkylidyne Chain Growth. The Crystal Structure of $Ru_3(\mu\text{-SEt})(\mu_3\text{-}\eta^3\text{-CCPhCHPh})(CO)_9$

Joseph W. Ziller, David K. Bower, Dennis M. Dalton, Jerome B. Keister,*[1] and Melvyn Rowen Churchill*

Department of Chemistry, University at Buffalo, State University of New York, Buffalo, New York 14214

Received July 25, 1988

The reaction of $(\mu\text{-H})_3Ru_3(\mu_3\text{-CSEt})(CO)_9$ with alkynes C_2R_2 (R = Me or Ph) gives two isomeric alkylidyne–alkyne coupled products: $(\mu\text{-H})Ru_3(\mu_3\text{-}\eta^3\text{-EtSCCRCR})(CO)_9$, containing a 1,3-dimetalloallyl ligand, and $Ru_3(\mu\text{-SEt})(\mu_3\text{-}\eta^3\text{-CCRCHR})(CO)_9$, containing a 1,1-dimetalloallyl ligand. All clusters were characterized by spectroscopic methods; additionally, the structure of $Ru_3(\mu\text{-SEt})(\mu_3\text{-}\eta^3\text{-CCPhCHPh})(CO)_9$ was determined by X-ray crystallography. $Ru_3(\mu\text{-SEt})(\mu_3\text{-}\eta^3\text{-CCPhCHPh})(CO)_9$ crystallizes in the centrosymmetric triclinic space group $P\bar{1}$, with a = 10.0719 (13) Å, b = 11.6576 (15) Å, c = 13.1047 (17) Å, α = 78.319 (11)°, β = 76.647 (10)°, γ = 76.225 (11)°, V = 1436.2 (2) Å^3, and Z = 2. Diffraction data (Mo Kα, 2θ = 4.0–45.0°) were collected with a Syntex $P2_1$ diffractometer, and the structure was solved and refined to R_F = 5.5% and R_{wF} = 3.7% for 3774 data (R_F = 2.9%, R_{wF} = 3.0% for those 2702 reflections with $|F_o| > 6.0\sigma(|F_o|)$). The molecule is a 50-electron cluster with Ru(1)–Ru(2) = 2.759 (1) Å, Ru(1)–Ru(3) = 2.887 (1) Å, and ∠Ru(2)–Ru(1)–Ru(3) = 90.72 (2)°. Each ruthenium atom bears three CO ligands. The μ-SEt ligand bridges two Ru atoms with Ru(1)–S = 2.433 (2) Å, Ru(2)–S = 2.376 (2) Å, and ∠Ru(1)–S–Ru(2) = 69.99 (5)°. The $\mu_3\text{-}\eta^3$-CC(Ph)CHPh ligand is σ-bonded to Ru(1) and Ru(2) (Ru(1)–C(1) = 2.188 (6) Å and Ru(2)–C(1) = 2.039 (6) Å) and is bonded via an η^3-allyl system to Ru(3) [Ru(3)–C(1) = 2.155 (6) Å, Ru(3)–C(4) = 2.225 (6) Å, Ru(3)–C(5) = 2.250 (6) Å, and ∠C(1)–C(4)–C(5) = 117.6 (6)°]. $(\mu\text{-H})Ru_3(\mu_3\text{-}\eta^3\text{-EtSCCRCR})(CO)_9$ isomerizes to $Ru_3(\mu\text{-SEt})(\mu_3\text{-}\eta^3\text{-CCRCHR})(CO)_9$ in quantitative yield with a first-order rate law (k, 7.9 × 10^{-5} s^{-1} (R = Me) at 60 °C). The isomerization of $(\mu\text{-H})Ru_3(\mu_3\text{-}\eta^3\text{-EtSCCRCR})(CO)_9$ to $Ru_3(\mu\text{-SEt})(\mu_3\text{-}\eta^3\text{-CCRCHR})(CO)_9$ involves two of the steps that occur during the related hydrogenation of $(\mu\text{-H})Ru_3(\mu_3\text{-}\eta^3\text{-XCCRCR})(CO)_9$ (X = OMe or SEt) to $(\mu\text{-H})_3Ru_3(\mu_3\text{-CCHRCH}_2\text{R})(CO)_9$. Hydrogenation of $Ru_3(\mu\text{-SEt})(\mu_3\text{-}\eta^3\text{-CCMeCHMe})(CO)_9$ (4 atm, 70 °C) forms $(\mu\text{-H})_3Ru_3(\mu_3\text{-CCHMeCH}_2\text{Me})(CO)_9$ (4%) and $(\mu\text{-H})Ru_3(\mu\text{-SEt})(CO)_{10}$ (51%). The overall conversion of $(\mu\text{-H})_3Ru_3(\mu_3\text{-CSEt})(CO)_9$ to $(\mu\text{-H})_3Ru_3(\mu_3\text{-CCHRCH}_2\text{R})(CO)_9$ is an example of cluster-centered hydrocarbon chain growth.

Carbon-carbon bond formation between an alkylidyne fragment and an alkyne has been observed in a number of cluster systems.[2,3] Several years ago we reported the coupling of alkynes with the alkylidyne ligand of $(\mu\text{-H})_3Ru_3(\mu_3\text{-CX})(CO)_9$ (R = alkyl, aryl, OMe), forming $(\mu\text{-H})Ru_3(\mu_3\text{-}\eta^3\text{-XCCRCR})(CO)_9$, which contain a 1,3-dimetalloallyl ligand; when X = OMe, these products react with hydrogen to form alkylidyne-containing clusters of the general formula $(\mu\text{-H})_3Ru_3(\mu_3\text{-CCHRCH}_2\text{R})(CO)_9$.[3] The overall conversion of $(\mu\text{-H})_3Ru_3(\mu_3\text{-COMe})(CO)_9$ to $(\mu\text{-H})_3Ru_3(\mu_3\text{-CCHRCH}_2\text{R})(CO)_9$ is an example of cluster-centered hydrocarbon chain growth which may serve as a model for hydrocarbon coupling processes occurring on metal surfaces.

The analogous reaction between $(\mu\text{-H})_3Ru_3(\mu_3\text{-CSEt})(CO)_9$ and C_2R_2 (R = Me or Ph) was subsequently shown by two of us to give two isomeric products, the expected $(\mu\text{-H})Ru_3(\mu_3\text{-}\eta^3\text{-EtSCCRCR})(CO)_9$ and a new cluster, characterized in a preliminary communication as $Ru_3(CSEt)(CR{=}CHR)(CO)_9$ on the basis of spectroscopic data.[4]

We have now characterized, by X-ray crystallography for R = Ph, the latter isomer as $Ru_3(\mu\text{-SEt})(\mu_3\text{-}\eta^3\text{-CCRCHR})(CO)_9$, which contains a 1,1-dimetalloallyl ligand. Furthermore, we show that $(\mu\text{-H})Ru_3(\mu_3\text{-}\eta^3\text{-EtSCCRCR})(CO)_9$ can be thermally isomerized to $Ru_3(\mu\text{-SEt})(\mu_3\text{-}\eta^3\text{-CCRCHR})(CO)_9$, which in turn can be hydrogenated to form $(\mu\text{-H})Ru_3(\mu\text{-SEt})(CO)_{10}$ and the chain-growth product $(\mu\text{-H})_3Ru_3(\mu_3\text{-CCHRCH}_2\text{R})(CO)_9$. The complete reaction sequence is presented in Figure 1.

Experimental Section

General Data. Infrared spectra were recorded on a Beckman 4250 spectrophotometer. ^{1}H NMR spectra were recorded on a Varian EM-390 or JEOL FX-90Q instrument. ^{13}C NMR spectra were recorded on a JEOL FX-90Q 90 MHz or Varian Gemini 300 MHz spectrometer; $Cr(acac)_3$ was added as a relaxation agent. Mass spectra were obtained on a VG 70SE instrument at the University at Buffalo or were provided by the Penn State University Mass Spectrometry Laboratory; elemental composition was verified by comparison of experimental spectra with spectra calculated by using the program MSCALC, adapted by J. B. Keister from MASPAN[5] for use with IBM PC computers. Elemental analyses were performed by Schwarzkopf Microanalytical Laboratory.

(1) Alfred P. Sloan Fellow, 1987–1989.

(2) (a) Jeffery, J. C.; Went, M. J. *Polyhedron* **1988**, *7*, 775. (b) Clauss, A. D.; Shapley, J. R.; Wilson, S. R. *J. Am. Chem. Soc.* **1981**, *103*, 7387. (c) Nuel, D.; Dahan, F.; Mathieu, R. *J. Am. Chem. Soc.* **1985**, 107, 1658. (d) Nuel, D.; Mathieu, R. *Organometallics* **1988**, *7*, 16. (e) Kalam-Alami, M.; Mathieu, R. *J. Organomet. Chem.* **1986**, *299*, 363. (f) Dyke, A. F.; Knox, S. A. R.; Naish, P. J.; Taylor, G. E. *J. Chem. Soc., Dalton Trans.* **1982**, 1297. (g) Finnimore, S. R.; Knox, S. A. R.; Taylor, G. E. *Ibid.* **1982**, 1783.

(3) Beanan, L. R.; Keister, J. B. *Organometallics* **1985**, *4*, 1713.

(4) Dalton, D. M.; Keister, J. B. *J. Organomet. Chem.* **1985**, *290*, C37.

(5) (a) Knox, S. A. R.; Koepke, J. W.; Andrews, M. A.; Kaesz, H. D. *J. Am. Chem. Soc.* **1975**, *97*, 3942. (b) Andrews, M. A. Ph.D. Dissertation, University of California, Los Angeles, Los Angeles, CA, 1977.

0276-7333/89/2308-0492$01.50/0

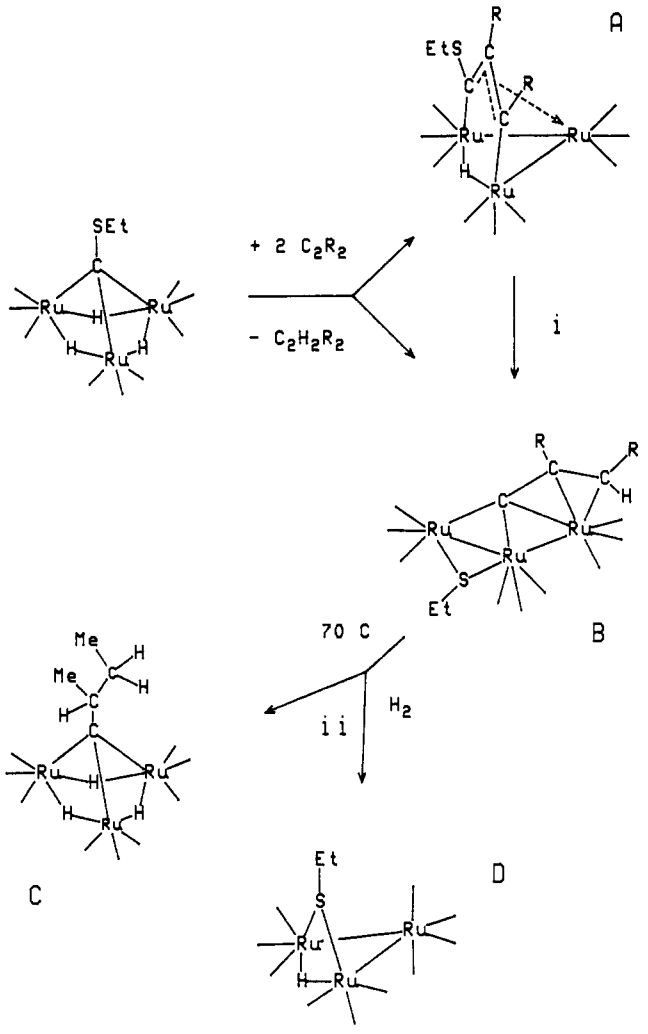

Figure 1. Reaction scheme converting $(\mu\text{-H})_3Ru_3(\mu_3\text{-CSEt})(CO)_9$ and C_2R_2 (R = Me or Ph) to $(\mu\text{-H})Ru_3(\mu_3\text{-}\eta^3\text{-EtSCCRCR})(CO)_9$ (structure A), which in turn is isomerized to $Ru_3(\mu\text{-SEt})(\mu_3\text{-}\eta^3\text{-CCRCHR})(CO)_9$ (structure B). Hydrogenation of B (R = Me) gives $(\mu\text{-H})_3Ru_3(\mu_3\text{-CCHMeCH}_2\text{Me})(CO)_9$ (structure C) and $(\mu\text{-H})Ru_3(\mu\text{-SEt})(CO)_{10}$ (structure D).

Starting Materials. $(\mu\text{-H})_3Ru_3(\mu_3\text{-CSEt})(CO)_9$[6] was prepared by using a previously published procedure.

Reaction of $(\mu\text{-H})_3Ru_3(\mu_3\text{-CSEt})(CO)_9$ with Diphenylacetylene. A solution of $(\mu\text{-H})_3Ru_3(\mu_3\text{-CSEt})(CO)_9$ (73 mg, 0.12 mmol) and diphenylacetylene (75 mg, 0.42 mmol) in cyclohexane was stirred under nitrogen for 21 h. The solution was then evaporated to dryness, and the residue was separated by thin-layer chromatography on silica eluting with hexanes. Three bands were obtained, in order of elution: yellow, 24 mg, $Ru_3(\mu\text{-SEt})(\mu_3\text{-}\eta^3\text{-CCPhCHPh})(CO)_9$; orange, 27 mg, $(\mu\text{-H})Ru_3(\mu_3\text{-}\eta^3\text{-EtSCCPhCPh})(CO)_9$; red-orange mixture of several components, 39.5 mg. Bands 1 and 2 were recrystallized from methanol to give analytically pure samples. Band 3 was separated by TLC on silica, eluting with 1:4 dichloromethane–hexanes; at least four bands were obtained and these were not examined further.

$Ru_3(\mu\text{-SEt})(\mu_3\text{-}\eta^3\text{-CCPhCHPh})(CO)_9$: IR ($C_6H_{12}$) 2076 w, 2062 s, 2042 s, 2021 s, 2006 s, 2000 m, 1984 w cm^{-1}; ^1H NMR ($CDCl_3$, 25 °C): 1.38 (t, 3 H_a), 2.71 (q, 2 H_b), 3.27 (s, 1 H), 7.0 (m, 10 H) ppm, J_{ab} = 7 Hz; ^{13}C NMR ($CDCl_3$, 25 °C) 274.0 (1 C, s), 196.7 (1 C, s), 196.2 (3 C, s), 195.6 (br, 3 C), 193.9 (1 C, s), 192.7 (1 C, s), 141.8 (1 C, s), 140.8 (1 C, s), 131.4 (2 C, d, J = 160 Hz), 128.9 (2 C, d, J = 160 Hz), 128.2 (br, 5 C, d, J = 160 Hz), 126.0 (1 C, d, J = 160 Hz), 117.8 (1 C, s), 55.6 (1 C, d, J = 158 Hz), 35.6 (1 C, t, J = 141 Hz), 19.0 (1 C, q, J = 130 Hz) ppm; EI MS, m/z 810 ($^{102}Ru_3$). Anal. Calcd for $C_{26}H_{16}O_9Ru_3S$: C, 38.66; H, 2.00. Found: C, 38.15; H, 2.14.

$(\mu\text{-H})Ru_3(\mu_3\text{-}\eta^3\text{-EtSCCPhCPh})(CO)_9$: IR ($C_6H_{12}$) 2098 m, 2076 s, 2062 m, 2040 s, 2033 sh, 2009 m, 2001 m, 1990 m, 1982 m cm^{-1}; ^1H NMR ($CDCl_3$, 25 °C) 7.1 (m, 10 H), 2.25 (q, 1 H_a), 1.95 (q, 1 H_b), 0.90 (t, 3 H_c), -19.93 (s, 1 H) ppm, $J_{ac,bc}$ = 7.3 Hz; EI MS, m/z 810 ($^{102}Ru_3$). Anal. Calcd for $C_{26}H_{16}O_9Ru_3S$: C, 38.66; H, 2.00. Found: C, 38.36; H, 2.16.

Reaction of $(\mu\text{-H})_3Ru_3(\mu_3\text{-CSEt})(CO)_9$ with 2-Butyne. A solution of $(\mu\text{-H})_3Ru_3(\mu_3\text{-CSEt})(CO)_9$ (62 mg, 0.099 mmol) and 2-butyne (74 mg, 1.4 mmol) in cyclohexane (5 mL) was stirred under a nitrogen atmosphere for 24 h. The solvent was then evaporated to dryness, and the residue was separated by thin-layer chromatography on silica eluting with hexanes. Five bands were eluted, in order of decreasing R_f: band 1, yellow, 7 mg, $Ru_3(\mu\text{-SEt})(\mu_3\text{-}\eta^3\text{-CCMeCHMe})(CO)_9$; band 2, yellow, 1 mg; band 3, orange, 30 mg, $(\mu\text{-H})Ru_3(\mu_3\text{-}\eta^3\text{-EtSCCMeCMe})(CO)_9$; bands 4 and 5, red-brown, total 10 mg.

$Ru_3(\mu\text{-SEt})(\mu_3\text{-}\eta^3\text{-CCMeCHMe})(CO)_9$: IR ($C_6H_{12}$) 2080 w, 2071 w, 2058 vs, 2041 s, 2009 vs, 2001 vs, 1994 vs, 1989 m, 1985 m cm^{-1}; ^1H NMR ($CDCl_3$, 25 °C) 2.66 (m, 2 $H_{a,a'}$), 2.35 (s, 3 H), 2.20 (q, 1 H_b), 1.78 (d, 3 H_c), 1.35 (t, 3 H_d) ppm, J_{ad} = 7.3 Hz, J_{bc} = 5.3 Hz; ^{13}C NMR ($CDCl_3$, 25 °C) 267.8 (s, 1 C), 197.2 (s, 1 C), 196.3 (s, 3 C), 196.0 (br, 3 C), 195.3 (s, 1 C), 193.4 (s, 1 C), 112.6 (s, 1 C), 51.2 (d, 1 C, J_{CH} = 158 Hz), 35.5 (t, 1 C, J_{CH} = 135 Hz), 26.4 (q, 1 C, J_{CH} = 128 Hz), 19.0 (q, 1 C, J_{CH} = 126 Hz), 18.6 (q, 1 C, J_{CH} = 126 Hz); ^{13}C NMR (-60 °C, carbonyl region (205–190 ppm) only) 200.8 (s, 1 C), 197.1 (s, 1 C), 196.2 (br, 3 C), 195.5 (s, 1 C), 195.2 (s, 1 C), 193.4 (s, 1 C), 191.8 (s, 1 C) ppm; EI MS, m/z 686 ($^{102}Ru_3$).

$(\mu\text{-H})Ru_3(\mu_3\text{-}\eta^3\text{-EtSCCMeCMe})(CO)_9$: IR ($C_6H_{12}$) 2095 w, 2074 m, 2063 w, 2038 s, 2021 w, 2006 s, 1989 m, 1976 m cm^{-1}; ^1H NMR ($CDCl_3$, 25 °C) 2.87 (s, 3 H), 2.42 (s, 3 H), 2.30 (m, 1 H_a), 1.78 (m, 1 H_b), 1.38 (t, 3 H_c), -20.23 (s, 1 H) ppm, $J_{ab,ac}$ = 7.3 Hz; ^{13}C NMR ($CDCl_3$, 25 °C) 198.1 (3 C, s), 196.4 (1 C, d, J_{CH} = 2 Hz), 196.0 (1 C, s), 193.8 (1 C, s), 192.4 (1 C, d, J_{CH} = 4 Hz), 190.4 (1 C, d, J_{CH} = 13 Hz), 188.4 (1 C, d, J = 14 Hz), 186.9 (1 C, d, J_{CH} = 3 Hz), 182.2 (1 C, s), 131.1 (1 C, s), 40.4 (1 C, q, J_{CH} = 127 Hz), 37.4 (1 C, t, J_{CH} = 142 Hz), 22.9 (1 C, q, J_{CH} = 129 Hz), 13.8 (1 C, q, J_{CH} = 128 Hz) ppm; EI MS, m/z 686 ($^{102}Ru_3$). Anal. Calcd for $C_{16}H_{12}O_9Ru_3S$: C, 28.12; H, 1.77. Found: C, 27.91; H, 1.75.

Kinetics of Isomerization of $(\mu\text{-H})Ru_3(\mu_3\text{-}\eta^3\text{-EtSCCMeCMe})(CO)_9$ to $Ru_3(\mu\text{-SEt})(\mu_3\text{-}\eta^3\text{-CCMeCHMe})(CO)_9$. The progress of the isomerization reaction, conducted in heptane or decane solution, was monitored by IR spectroscopy, using a Beckman 4250 spectrophotometer and 0.5-mm KBr solution cells. Reactions were conducted in jacketed, glass vessels under a nitrogen or carbon monoxide atmosphere. The temperature was maintained to ±0.1° with a Neslab circulator bath. Samples were periodically withdrawn via glass pipet.

The rate constant for each run was determined by a computer-calculated (KINPLOT program written by Dr. R. Ruszczyk) least-squares determination of the slope of the plot of the ln (absorbance) vs time, using the peak at 2095 cm^{-1} of the starting material. Good linear plots were obtained for greater than 3 half-lives. At least three runs were made in each case; error limits are reported as the standard deviation from the mean.

Reaction of $Ru_3(\mu\text{-SEt})(\mu_3\text{-}\eta^3\text{-CCMeCHMe})(CO)_9$ with Hydrogen. A solution of $Ru_3(\mu\text{-SEt})(\mu_3\text{-}\eta^3\text{-CCMeCHMe})(CO)_9$ (350 mg, 0.512 mmol) in cyclohexane (40 mL) was placed in a Parr pressure bottle, which was then sealed and flushed with hydrogen. The bottle was pressurized to 4 atm with hydrogen and was heated in an oil bath at 75 °C for 1 h. The solution was then evaporated to dryness by using a rotary evaporator, and the residue was separated by using thin-layer chromatography on silica, eluting with hexanes. Three bands were eluted, in order of decreasing R_f: $(\mu\text{-H})_3Ru_3(\mu_3\text{-CCHMeCH}_2\text{Me})(CO)_9$ (14 mg, 4.4%), $(\mu\text{-H})Ru_3(\mu\text{-SEt})(CO)_{10}$ (169 mg, 51%), and a reddish brown band comprised of a number of components which were not characterized. $(\mu\text{-H})_3Ru_3(\mu_3\text{-CCHMeCH}_2\text{Me})(CO)_9$ and $(\mu\text{-H})Ru_3(\mu\text{-SEt})(CO)_{10}$ were characterized by comparing their IR, ^1H NMR, and mass spectra with those of authentic samples prepared by literature methods.[3,7]

(6) Churchill, M. R.; Ziller, J. W.; Dalton, D. M.; Keister, J. B. *Organometallics* **1987**, *6*, 806.

(7) Crooks, G. R.; Johnson, B. F. G.; Lewis, J.; Williams, I. G. *J. Chem. Soc. A* **1969**, 797.

Table I. Experimental Data for the X-ray Diffraction Study of $Ru_3(\mu\text{-SEt})(\mu_3\text{-}\eta^3\text{-CCPhCHPh})(CO)_9$

(A) Crystal Parameters at 21 °C (294 K)

cryst system: triclinic	space group: $P\bar{1}$ (C_i^1; No. 2)
a = 10.0719 (13) Å	V = 1436.2 (3) Å^3
b = 11.6576 (15) Å	formula: $C_{26}H_{16}O_9Ru_3S$
c = 13.1047 (17) Å	MW 807.7
α = 78.319 (11)°	Z = 2
β = 76.647 (10)°	D(calcd) = 1.87 g/cm^3
γ = 76.225 (11)°	

(B) Data Collection

diffractometer: Syntex $P2_1$
radiation: Mo Kα ($\bar{\lambda}$ = 0.710 730 Å)
monochromator: pyrolytic graphite, equatorial geometry, assumed to be 50% perfect/50% ideally mosaic for polarization correction
reflctns measd: $+h,\pm k,\pm l$ for 2θ = 4.0–45.0°; 4031 total reflections were merged to 3774 unique independent data; none rejected
scan type: coupled θ(crystal)–2θ(counter)
scan width: [2θ(Mo Kα_1) – 0.9] → [2θ(Mo Kα_2) + 0.9]°
scan speed: 4.0 deg /min
bkgd measurement: stationary crystal and stationary counter at each end of the 2θ scan; each for one-half total scan time
std reflctns: 3 ($54\bar{1}$, $2\bar{1}7$, $17\bar{3}$) remeasured after each batch of 97 reflections; no significant decay nor fluctuations were observed
absorptn correctn: μ(Mo Kα) = 16.4 cm^{-1}; corrected by interpolation in 2θ and ϕ between ψ-scans of three close-to-axial reflections (623, 511, 412)

Collection of X-ray Diffraction Data for $Ru_3(\mu\text{-SEt})(\mu_3\text{-}\eta^3\text{-CCPhCHPh})(CO)_9$. A bright yellow crystal of approximate dimensions 0.1 × 0.2 × 0.3 mm^3 was sealed into a thin-walled glass capillary and inserted into an aluminum pin. The pin was set in an XYZ goniometer and mounted on a Syntex $P2_1$ automated four-circle diffractometer. Crystal alignment, determination of the unit cell parameters and orientation matrix, and data collection were carried out as described previously;[8] details appear in Table I. The diffraction symmetry is $\bar{1}$ (C_i), and there are no systematic absences. The crystal belongs to the triclinic system. On the basis of intensity statistics and with Z = 2, it was assigned to the more probable centrosymmetric triclinic space group $P\bar{1}$ (C_i^1; No. 2). Successful solution of the structure under this higher symmetry space group proves it to be the correct choice.

All data were corrected for the effects of absorption and for Lorentz and polarization effects, were converted to unscaled $|F_o|$ values, and were placed on an approximate absolute scale by means of a Wilson plot. Any reflection with I(net) < 0 was assigned the value $|F_o|$ = 0. The $10\bar{1}$ reflection was deemed unreliable due to "clipping" by the backstop and was rejected.

Solution and Refinement of the Crystal Structure. All crystallographic calculations were performed on the University at Buffalo-SUNY modified version of the Syntex XTL structure solution package. The analytical form of the appropriate neutral atom's scattering factor was corrected for both the real ($\Delta f'$) and imaginary ($i\Delta f''$) components of anomalous dispersion.[9] The function minimized during least-squares refinement was $\sum w(|F_o| - |F_c|)^2$, where $1/w = [(\sigma|F_o|)^2 + (0.015|F_o|)^2]$.

The positions of the three ruthenium atoms were derived from a combination of sharpened and unsharpened three-dimensional Patterson maps. All remaining atoms (including hydrogen atoms) were located from a series of difference-Fourier syntheses. Full-matrix least-squares refinement of positional and thermal parameters (anisotropic for all non-hydrogen atoms) led to convergence[10] with R_F = 5.5%, R_{wF} = 3.7%, and GOF = 1.13 for 416 variables refined against 3774 unique data. Residual for those 3099 reflections with $|F_o| > 3\sigma(|F_o|)$ were R_F = 3.7% and R_{wF} = 3.4%, and for those 2702 reflections with $|F_o| > 6\sigma(|F_o|)$, R_F = 2.9% and R_{wF} = 3.0%. Final positional and isotropic thermal parameters are collected in Table II. Anisotropic thermal parameters are given in the supplementary material (Table 2S).

(8) Churchill, M. R.; Lashewycz, R. A.; Rotella, F. J. *Inorg. Chem.* **1977**, *16*, 265.
(9) *International Tables for X-Ray Crystallography*; Kynoch: Birmingham, England, 1974; Vol. 4, pp 99–101, 149–150.
(10) R_F (%) = $100\sum||F_o| - |F_c||/\sum|F_o|$; R_{wF} (%) = $100[\sum w(|F_o| - |F_c|)^2/\sum w|F_o|^2]^{1/2}$; GOF = $[\sum w(|F_o| - |F_c|)^2/(NO - NV)]^{1/2}$, where NO = number of observations and NV = number of variables.

Table II. Final Positional Parameters with Esd's for $Ru_3(\mu\text{-SEt})(\mu_3\text{-}\eta^3\text{-CCPhCHPh})(CO)_9$

atom	x	y	z
Ru(1)	0.38105 (5)	0.48970 (5)	0.23566 (4)
Ru(2)	0.13676 (5)	0.49095 (5)	0.17381 (4)
Ru(3)	0.36260 (5)	0.26563 (5)	0.37496 (4)
S	0.14650 (18)	0.55936 (15)	0.33036 (14)
C(2)	0.0947 (10)	0.72216 (70)	0.32164 (71)
C(3)	0.1198 (18)	0.7598 (11)	0.4163 (10)
O(11)	0.65017 (58)	0.38737 (48)	0.09434 (42)
O(12)	0.38671 (61)	0.73046 (49)	0.08982 (45)
O(13)	0.54417 (58)	0.53459 (47)	0.38891 (42)
O(21)	0.05658 (60)	0.74472 (51)	0.04797 (46)
O(22)	0.21659 (64)	0.37250 (51)	–0.02494 (45)
O(23)	–0.15075 (56)	0.42721 (57)	0.24567 (49)
O(31)	0.20188 (52)	0.39714 (47)	0.56190 (40)
O(32)	0.28749 (72)	0.05090 (52)	0.53398 (46)
O(33)	0.65171 (57)	0.23359 (50)	0.42629 (44)
C(11)	0.54749 (76)	0.42194 (59)	0.14595 (54)
C(12)	0.38053 (74)	0.64155 (67)	0.14412 (58)
C(13)	0.48378 (71)	0.51524 (56)	0.33443 (54)
C(21)	0.08230 (75)	0.65256 (69)	0.09415 (60)
C(22)	0.18260 (72)	0.41861 (63)	0.04909 (60)
C(23)	–0.04440 (83)	0.45223 (65)	0.21723 (61)
C(31)	0.25520 (68)	0.35669 (59)	0.48763 (56)
C(32)	0.31925 (77)	0.12824 (69)	0.47161 (59)
C(33)	0.54227 (77)	0.24587 (62)	0.40954 (54)
C(1)	0.26971 (61)	0.34882 (52)	0.23863 (47)
C(4)	0.31271 (60)	0.22723 (52)	0.23006 (45)
C(41)	0.20854 (68)	0.15640 (55)	0.22261 (51)
C(42)	0.23339 (86)	0.09546 (62)	0.13887 (62)
C(43)	0.1399 (13)	0.03287 (81)	0.1262 (10)
C(44)	0.0189 (13)	0.03291 (89)	0.1972 (12)
C(45)	–0.0123 (10)	0.09379 (88)	0.2808 (11)
C(46)	0.08434 (77)	0.15592 (68)	0.29498 (71)
C(5)	0.45555 (66)	0.17367 (56)	0.23198 (50)
C(51)	0.51782 (65)	0.04168 (56)	0.23626 (50)
C(52)	0.45200 (80)	–0.04904 (63)	0.29589 (57)
C(53)	0.5161 (10)	–0.16816 (68)	0.29565 (67)
C(54)	0.64657 (93)	–0.19960 (72)	0.23530 (70)
C(55)	0.71115 (88)	–0.10981 (79)	0.17548 (74)
C(56)	0.64942 (74)	0.00895 (67)	0.17655 (64)

atom	x	y	z	B(iso), Å^2
H(21)	–0.0053 (70)	0.7345 (55)	0.3167 (47)	5.0 (16)
H(22)	0.1408 (70)	0.7611 (60)	0.2643 (54)	4.2 (19)
H(31)	0.0894 (68)	0.6450 (67)	0.4095 (51)	4.8 (17)
H(32)	0.0632 (91)	0.7247 (80)	0.4869 (73)	8.1 (28)
H(33)	0.204 (13)	0.736 (11)	0.427 (10)	11.3 (52)
H(5)	0.5175 (63)	0.2197 (54)	0.1998 (47)	3.2 (15)
H(42)	0.3228 (61)	0.0920 (50)	0.0910 (44)	2.6 (14)
H(43)	0.1579 (83)	–0.0156 (73)	0.0773 (63)	6.7 (24)
H(44)	–0.0373 (93)	–0.0059 (80)	0.1856 (70)	8.2 (28)
H(45)	–0.0782 (93)	0.0968 (81)	0.3273 (71)	7.0 (29)
H(46)	0.0631 (65)	0.1997 (58)	0.3519 (50)	3.5 (17)
H(52)	0.3662 (69)	–0.0215 (58)	0.3385 (51)	4.4 (17)
H(53)	0.4643 (65)	–0.2251 (59)	0.3321 (50)	3.9 (17)
H(54)	0.6909 (78)	–0.2914 (74)	0.2314 (58)	7.0 (20)
H(55)	0.8006 (58)	–0.1268 (47)	0.1368 (41)	2.0 (12)
H(56)	0.6964 (72)	0.0713 (63)	0.1298 (54)	6.0 (19)

Results

At room temperature $(\mu\text{-H})_3Ru_3(\mu_3\text{-CSEt})(CO)_9$ reacts with alkynes C_2R_2 (R = Me or Ph) to give two major, isomeric products. The relative amount of each isomer depends upon the time allowed for reaction to occur, since $(\mu\text{-H})Ru_3(\mu_3\text{-}\eta^3\text{-EtSCCRCR})(CO)_9$ slowly isomerizes to $Ru_3(\mu\text{-SEt})(\mu_3\text{-}\eta^3\text{-CCRCHR})(CO)_9$ (vide infra). The isomers are easily separated by using thin-layer chromatography.

The 1,3-dimetalloallyl clusters $(\mu\text{-H})Ru_3(\mu_3\text{-}\eta^3\text{-EtSCCRCR})(CO)_9$ (R = Me or Ph) are red-orange, air-stable, crystalline compounds, readily soluble in most or-

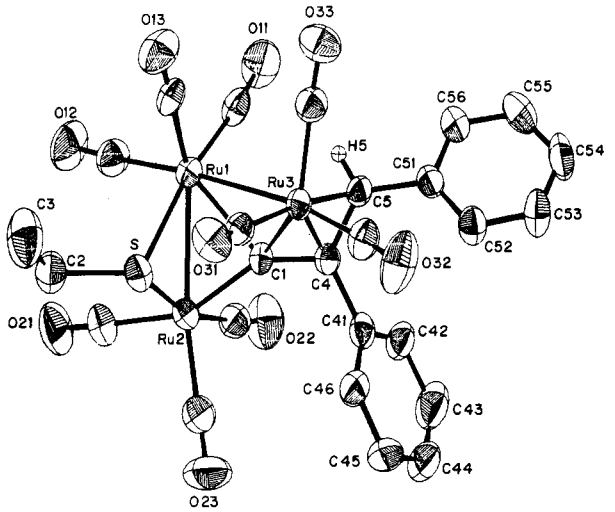

Figure 2. Labeling of atoms in the $Ru_3(\mu\text{-SEt})(\mu_3\text{-}\eta^3\text{-CCPhCHPh})(CO)_9$ molecule (ORTEP diagram; 30% probability ellipsoids). Hydrogen atoms on the phenyl and ethyl groups are omitted.

ganic solvents. The compounds (Figure 1, structure A) were characterized by comparison of their IR, ^1H and ^{13}C NMR (for R = Me), and mass spectra with those of previously characterized analogues, such as $(\mu\text{-H})Ru_3(\mu_3\text{-}\eta^3\text{-MeOCCRCR})(CO)_9$[3] and $(\mu\text{-H})Ru_3(\mu_3\text{-}\eta^3\text{-EtCCHCMe})(CO)_9$.[11] The molecular ion and ions derived by sequential loss of CO ligands from the molecular ion are observed in the EI mass spectra. The IR spectra display only terminal CO stretching frequencies. The ^1H NMR spectra are quite similar to those of analogous $(\mu\text{-H})Ru_3(\mu_3\text{-}\eta^3\text{-MeOCCRCR})(CO)_9$[3] clusters; the hydride resonance at ca. −20 ppm is characteristic. The ^{13}C NMR spectrum of $(\mu\text{-H})Ru_3(\mu_3\text{-}\eta^3\text{-EtSCCMeCMe})(CO)_9$ can be assigned by comparison with that of $(\mu\text{-H})Ru_3(\mu_3\text{-}\eta^3\text{-HCCMeCMe})(CO)_9$.[12] In the ^{13}C spectrum of $(\mu\text{-H})Ru_3(\mu_3\text{-}\eta^3\text{-HCCMeCMe})(CO)_9$ the resonances for the allylic 2-carbon and the attached methyl group occur at 130.4 and 27.0 ppm, respectively; the resonance for the 3-carbon and the attached methyl group occur at 186.8 and 37.6 ppm, respectively. Thus, for $(\mu\text{-H})Ru_3(\mu_3\text{-}\eta^3\text{-EtSCCMeCMe})(CO)_9$, the resonance at 131.1 ppm is assigned to the 2-carbon and the resonance for the 2-methyl group at 22.9 ppm. We assign the resonance at 186.9 ppm to the 3-carbon and the one at 40.4 ppm to the attached methyl group. The assignment of the 1-carbon resonance is ambiguous but is most likely 182.2 ppm. As found for other clusters of this class, threefold fluxional exchange averages the resonances (198.1 ppm) due to the three CO ligands coordinated to the Ru atom which is π bound to the allyl unit. On the basis of the magnitude of the C–H coupling constants, the resonances at 190.4 and 188.4 ppm can be assigned to the CO ligands trans to the bridging hydride.

The structure of $Ru_3(\mu\text{-SEt})(\mu_3\text{-}\eta^3\text{-CCRCHR})(CO)_9$ (R = Me or Ph) could not be determined by spectroscopic methods; however, the spectroscopic data are consistent with the solid-state structure, determined by X-ray crystallography, for R = Ph (Figure 2). The molecular ion and ions derived by stepwise loss of CO ligands are observed in the EI mass spectra. The IR spectra exhibit terminal CO stretches. For each compound, the ^1H NMR spectrum consists of resonances due to the ethyl group, resonances for nonequivalent R groups from the alkyne, a single allylic proton (coupled to the protons of the methyl group), and no hydride resonance. The ^{13}C NMR spectrum for R = Me consists of resonances at 267.8 (s, 1 C) ppm, assigned to the alkylidyne carbon on the basis of its low field chemical shift, 112.6 (s, 1 C) ppm, assigned to the 2-carbon atom of the 1,1-dimetalloallyl ligand, 51.2 (d, 1 C, J_{CH} = 158 Hz) ppm, assigned to the 3-carbon of the 1,1-dimetalloallyl ligand, 35.5 (t, 1 C, J_{CH} = 135 Hz) ppm, assigned to the methylene carbon of the thiolate ligand, and methyl carbon resonances at 26.4 (q, 1 C, J_{CH} = 128 Hz), 19.0 (q, 1 C, J_{CH} = 126 Hz), and 18.6 (q, 1 C, J_{CH} = 126 Hz) ppm; the CO resonances are observed at 197.2 (s, 1 C), 196.3 (s, 3 C), 196.0 (br, 3 C), 195.3 (s, 1 C), 193.4 (s, 1 C) ppm. At −60 °C the three CO ligands on one of the Ru atoms are still exchange-averaged (196.3 ppm), but the other six resonances show slow-exchange behavior (200.8, 197.1, 195.5, 195.2, 193.4, and 191.8 ppm).

Table III. Interatomic Distances (Å) and Esd's for $Ru_3(\mu\text{-SEt})(\mu_3\text{-}\eta^3\text{-CCPhCHPh})(CO)_9$

(A) Ruthenium–Ruthenium, Ruthenium–Sulfur, and Sulfur–Carbon Distances			
Ru(1)–Ru(2)	2.759 (1)	Ru(1)–Ru(3)	2.887 (1)
Ru(2)···Ru(3)	4.018 (1)	Ru(2)–S	2.376 (2)
Ru(1)–S	2.433 (2)	S–C(2)	1.832 (8)
(B) Ruthenium–Carbon (CO) and C–O Distances			
Ru(1)–C(11)	1.911 (7)	C(11)–O(11)	1.131 (9)
Ru(1)–C(12)	1.926 (8)	C(12)–O(12)	1.138 (9)
Ru(1)–C(13)	1.938 (7)	C(13)–O(13)	1.123 (9)
Ru(2)–C(21)	1.979 (8)	C(21)–O(21)	1.124 (10)
Ru(2)–C(22)	1.903 (7)	C(22)–O(22)	1.148 (9)
Ru(2)–C(23)	1.914 (9)	C(23)–O(23)	1.137 (11)
Ru(3)–C(31)	1.956 (7)	C(31)–O(31)	1.132 (9)
Ru(3)–C(32)	1.902 (8)	C(32)–O(32)	1.141 (10)
Ru(3)–C(33)	1.916 (8)	C(33)–O(33)	1.143 (10)
(C) Ruthenium–Carbon (μ_3-η^3-CCPhCHPh) Distances			
Ru(1)–C(1)	2.188 (6)	Ru(3)–C(4)	2.225 (6)
Ru(2)–C(1)	2.039 (6)	Ru(3)–C(5)	2.250 (6)
Ru(3)–C(1)	2.155 (6)	Ru(3)···H(5)	2.54 (6)
(D) Selected Carbon–Carbon Distances			
C(2)–C(3)	1.487 (17)		
C(1)–C(4)	1.400 (8)	C(4)–C(5)	1.429 (9)
C(4)–C(41)	1.512 (9)	C(5)–C(51)	1.512 (9)

Description of the Crystal and Molecular Structure of $Ru_3(\mu\text{-SEt})(\mu_3\text{-}\eta^3\text{-CCPhCHPh})(CO)_9$. The crystal contains an ordered racemic array of the two enantiomeric forms of the chiral $Ru_3(\mu\text{-SEt})(\mu_3\text{-}\eta^3\text{-CCPhCHPh})(CO)_9$ molecule, separated by normal van der Waals' distances; there are no abnormally short contacts between the molecular units. The overall molecular geometry and the scheme used to labelling atoms are illustrated in Figure 2. Interatomic distances and angles are collected in Tables III and IV. A stereoscopic view of the molecular appears as Figure 3 in the supplementary material.

The $Ru_3(\mu\text{-SEt})(\mu_3\text{-}\eta^3\text{-CCPhCHPh})(CO)_9$ molecule contains a bent, non-cyclic arrangement of ruthenium atoms. There is no direct interaction between atoms Ru(2) and Ru(3). Each ruthenium atom is in a different stereochemical environment and is linked to three terminal carbonyl ligands. Ru(1) and Ru(2) are bridged by the μ-SEt ligand and by C(1) and of the μ_3-η^3-CCPhCHPh ligand. The μ_3-η^3-CCPhCHPh ligand is coordinated to Ru(3) through a delocalized (η^3) π-allyl system.

The trinuclear arrangement is associated with the expected 50 outer valence electrons. (Using the neutral metal/neutral ligand electron counting method, we get 24 electrons from the three d^8 Ru(0) atoms, 18 electrons from the nine terminal carbonyl ligands, 3 electrons from the

(11) Evans, M.; Hursthouse, M.; Randall, E. W.; Rosenberg, E.; Milone, L.; Valle, M. *J. Chem. Soc., Chem. Commun.* **1972**, 545.
(12) Aime, S.; Milone, L.; Osella, D.; Valle, M.; Randall, E. W. *Inorg. Chim. Acta* **1976**, *20*, 217.

Table IV. Interatomic Angles (deg) and Esd's for $Ru_3(\mu\text{-SEt})(\mu_3\text{-}\eta^3\text{-CCPhCHPh})(CO)_9$

(A) Angles about the Ruthenium Atoms			
Ru(2)–Ru(1)–Ru(3)	90.72 (2)	S–Ru(2)–C(1)	79.7 (2)
Ru(2)–Ru(1)–S	54.04 (4)	Ru(1)–Ru(3)–C(1)	48.8 (2)
Ru(3)–Ru(1)–S	85.01 (5)	Ru(1)–Ru(3)–C(4)	79.6 (2)
Ru(1)–Ru(2)–S	55.97 (5)	Ru(1)–Ru(3)–C(5)	87.7 (2)
Ru(3)–Ru(1)–C(1)	47.9 (2)	C(1)–Ru(3)–C(4)	37.2 (2)
Ru(2)–Ru(1)–C(1)	47.0 (2)	C(1)–Ru(3)–C(5)	66.6 (2)
Ru(1)–Ru(2)–C(1)	51.6 (2)	C(4)–Ru(3)–C(5)	37.3 (2)
S–Ru(1)–C(1)	75.6 (2)		
(B) Ru–Ru–CO Angles			
Ru(2)–Ru(1)–C(11)	115.1 (2)	Ru(1)–Ru(2)–C(21)	106.0 (2)
Ru(2)–Ru(1)–C(12)	86.1 (2)	Ru(1)–Ru(2)–C(22)	108.3 (2)
Ru(2)–Ru(1)–C(13)	152.3 (2)	Ru(1)–Ru(2)–C(23)	145.9 (2)
Ru(3)–Ru(1)–C(11)	93.3 (2)	Ru(1)–Ru(3)–C(31)	88.4 (2)
Ru(3)–Ru(1)–C(12)	176.3 (2)	Ru(1)–Ru(3)–C(32)	170.8 (2)
Ru(3)–Ru(1)–C(13)	84.4 (2)	Ru(1)–Ru(3)–C(33)	94.1 (2)
(C) OC–Ru–CO and Ru–C–O Angles			
C(11)–Ru(1)–C(12)	89.7 (3)	Ru(1)–C(11)–O(11)	175.3 (7)
C(11)–Ru(1)–C(13)	92.4 (3)	Ru(1)–C(12)–O(12)	176.8 (7)
C(12)–Ru(1)–C(13)	97.6 (3)	Ru(1)–C(13)–O(13)	177.0 (6)
C(21)–Ru(2)–C(22)	92.6 (3)	Ru(2)–C(21)–O(21)	177.4 (7)
C(21)–Ru(2)–C(23)	97.9 (3)	Ru(2)–C(22)–O(22)	176.6 (7)
C(22)–Ru(2)–C(23)	94.3 (3)	Ru(2)–C(23)–O(23)	178.0 (7)
C(31)–Ru(3)–C(32)	85.8 (3)	Ru(3)–C(31)–O(31)	170.6 (6)
C(31)–Ru(3)–C(33)	97.4 (3)	Ru(3)–C(32)–O(32)	175.4 (7)
C(32)–Ru(3)–C(33)	93.7 (3)	Ru(3)–C(33)–O(33)	177.4 (7)
(D) OC–Ru–S, Ru–C–C, and Ru–S–C Angles			
C(11)–Ru(1)–S	168.9 (2)	Ru(2)–C(1)–C(4)	136.0 (5)
C(12)–Ru(1)–S	91.7 (2)	Ru(3)–C(1)–C(4)	74.1 (4)
C(13)–Ru(1)–S	98.4 (2)	Ru(3)–C(4)–C(1)	68.7 (4)
C(21)–Ru(2)–S	95.2 (2)	Ru(3)–C(4)–C(41)	128.4 (4)
C(22)–Ru(2)–S	163.9 (2)	Ru(3)–C(4)–C(5)	72.3 (4)
C(23)–Ru(2)–S	98.5 (2)	Ru(3)–C(5)–C(4)	70.4 (4)
Ru(1)–C(1)–C(4)	133.5 (5)	Ru(3)–C(5)–C(51)	124.8 (5)
Ru(1)–S–C(2)	114.3 (3)	Ru(2)–S–C(2)	112.9 (3)
(E) Selected Angles within the Bridging Ligands			
S–C(2)–C(3)	109.9 (8)	C(41)–C(4)–C(5)	122.5 (6)
C(1)–C(4)–C(41)	120.1 (5)	C(4)–C(5)–C(51)	125.4 (6)
C(1)–C(4)–C(5)	117.6 (6)	C(5)–C(51)–C(52)	124.5 (6)
C(4)–C(41)–C(42)	119.4 (6)	C(5)–C(51)–C(56)	117.8 (6)
C(4)–C(41)–C(46)	122.1 (6)	Ru(1)–S–Ru(2)	69.99 (5)

μ-SEt ligand, and 5 electrons from the μ_3-η^3-CCPhCHPh ligand). Electron counts at the individual metal atoms are inequivalent with $18^1/_2$e at Ru(1), $17^1/_2$e at Ru(2), and 18e at Ru(3). The two Ru–Ru linkages are inequivalent. That bridged by the μ-SEt ligand and C(1) of the π-allyl group, i.e. Ru(1)–Ru(2), is 2.759 (1) Å in length and is consistent with the thioether-bridged Ru–Ru linkage of 2.769 (1) Å found in $(\mu\text{-H})Ru_3(\mu_3\text{-}\eta^2\text{-}CH_2SEt)(CO)_9$.[6] The Ru(1)–Ru(3) linkage of 2.887 (1) Å is slightly longer than Ru–Ru(av) = 2.854 (5) Å in the parent binary carbonyl $Ru_3(CO)_{12}$.[13] The Ru(2)–Ru(1)–Ru(3) angle is 90.72 (2)°.

The μ-SEt ligand is associated with ruthenium-sulfur distances of Ru(1)–S = 2.433 (2) Å and Ru(2)–S = 2.376 (2) Å and an acute Ru(1)–S–Ru(2) angle of 69.99 (5)°. The slight difference in Ru–S distances may be due in part to the inequivalent electron counts at the individual metal atoms. The longer Ru–S bond is associated with the formally electron-rich Ru(1) center while the shorter bond is associated with the formally electron-poor Ru(2) center (this pattern is also seen in Ru–S distances in $(\mu\text{-H})Ru_3(\mu_3\text{-}\eta^2\text{-}CH_2SEt)(CO)_9$ (viz., Ru–S = 2.348 (2) and 2.302 (2) Å)[6] but not in $(\mu\text{-H})Ru_3(CO)_{10}(\mu\text{-SEt})$ (Ru–S = 2.389 (4) and 2.391 (4) Å),[14] where the electron counts at the sulfur-bound ruthenium atoms are equal). Alternatively, the SEt ligand may be considered to donate one electron to Ru(1) and two electrons to Ru(2), resulting in 18e counts for both metal atoms and rationalizing the longer Ru(1)–S bond distance. The S–C(2) distance of 1.832 (8) Å is normal.[15]

The μ_3-η^3-CCPhCHPh ligand is coordinated to the Ru_3 unit by σ-bonds from C(1) to both Ru(1) and Ru(2) (Ru(1)–C(1) = 2.188 (6) Å, Ru(2)–C(1) = 2.039 (6) Å) and by an η^3 π-bonding system from the C(1)–C(4)–C(5) allyl unit to Ru(3) (Ru(3)–C(1) = 2.155 (6) Å, Ru(3)–C(4) = 2.225 (6) Å, and Ru(3)–C(5) = 2.250 (6) Å). The Ru(1)–C(1)–Ru(2) angle is 81.4 (2)°. Although the Ru(3)–C(1) distance of 2.155 (6) Å is short, the Ru(3)–C(4) and Ru(3)–C(5) distances are consistent with the relatively imprecise value for the Ru–C(allyl) bond lengths of 2.22 (5) Å found in $(\mu\text{-H})Ru_3(\mu_3\text{-}\eta^3\text{-CMeCHCEt})(CO)_9$.[11] The C(1)–C(4) and C(4)–C(5) distances are 1.400 (8) and 1.429 (9) Å, respectively, and the C(1)–C(4)–C(5) angle is 117.6 (6)°. The carbon–carbon single bonds C(4)–C(41) and C(5)–C(51) are associated with identical distances (1.512 (9) Å). Carbon–carbon bond distances within the phenyl rings range from 1.352 (19) to 1.408 (13) Å. The refined C–H distances range from 0.79 (10) through 1.06 (9) Å, averaging 0.93 Å.

The individual Ru–CO distances range from 1.902 (8) through 1.979 (8) Å; the carbonyl ligands at a given ruthenium center are approximately mutually orthogonal to one another with OC–Ru–CO angles ranging from 85.8 (3)° to 97.9 (3)°. The C–O distances are uniform and lie in the range 1.123 (9) to 1.148 (9) Å.

Isomerization of $(\mu\text{-H})Ru_3(\mu_3\text{-}\eta^3\text{-EtSCCRCR})(CO)_9$ to $Ru_3(\mu\text{-SEt})(\mu_3\text{-}\eta^3\text{-CCRCHR})(CO)_9$. Slow isomerization of $(\mu\text{-H})Ru_3(\mu_3\text{-}\eta^3\text{-EtSCCRCR})(CO)_9$ to $Ru_3(\mu\text{-SEt})(\mu_3\text{-}\eta^3\text{-CCRCHR})(CO)_9$ occurs in solution at room temperature (Figure 1, reaction i). The isomerization is quantitative by IR spectroscopy, and isosbestic points are noted in the spectra during the course of the reaction, indicating the absence of a detectable concentration of any intermediate.

Preliminary measurements were made of the kinetics of the isomerization at 60 °C. Linear plots of ln (absorbance) for $(\mu\text{-H})Ru_3(\mu_3\text{-}\eta^3\text{-EtSCCMeCMe})(CO)_9$ vs time indicate that the rate law for the isomerization is first order. The first-order rate constant was found to be unaffected by the addition of CO ($8.2\ (\pm0.2) \times 10^{-5}$ s^{-1} under 1 atm of CO vs $7.9\ (\pm0.5) \times 10^{-5}$ s^{-1} under N_2), indicating that CO dissociation is not a factor in the rate-determining step. The rate constant for isomerization of $(\mu\text{-H})Ru_3(\mu_3\text{-}\eta^3\text{-EtSCCPhCPh})(CO)_9$ ($1.1\ (\pm0.03) \times 10^{-4}$ s^{-1} at 60.0 °C) was only slightly greater than that for isomerization of $(\mu\text{-H})Ru_3(\mu_3\text{-}\eta^3\text{-EtSCCMeCMe})(CO)_9$. The mechanism of the isomerization will be the subject of further studies.

Discussion

We have previously proposed that alkylidyne–alkylidyne coupling on metal surfaces to form alkynes and subsequent alkylidyne–alkyne coupling could give rise to surface-bound μ_3-η^3-XCCRCR (X = H, OH, or alkyl; R = H or alkyl) fragments in the Fischer–Tropsch reaction, which converts CO and hydrogen to linear and branched hydrocarbons. Indeed, the large number of examples of formation of this hydrocarbon fragment on molecular complexes makes it highly likely that the fragment will be important in many reactions occurring on metal surfaces. For this reason the mechanism of hydrogenation of the μ_3-η^3-XCCRCR ligand

(13) Churchill, M. R.; Hollander, F. J.; Hutchinson, J. P. *Inorg. Chem.* **1977**, *16*, 2655.
(14) Churchill, M. R.; Ziller, J. W.; Keister, J. B. *J. Organomet. Chem.* **1985**, *297*, 93.
(15) *Spec. Publ.—Chem. Soc.* **1965**, *No. 18*, S22s.
(16) (a) Rofer-DePoorter, C. K. *Chem. Rev.* **1981**, *81*, 447. (b) Muetterties, E. L.; Stein, J. *Chem. Rev.* **1979**, *79*, 479.

is of interest as a model for this metal surface chemistry.

In earlier work[3] we found that hydrogenation of (μ-H)Ru_3(μ_3-η^3-MeOCCRCR)$(CO)_9$ (R = H, alkyl, aryl, or CO_2Me) gave (μ-H)$_3Ru_3$(μ_3-CCHRCH$_2$R)$(CO)_9$ in modest yields (90 °C, 1–4 atm, 6–43%), in addition to the major product $H_4Ru_4(CO)_{12}$. The overall reaction is a complex one, involving C–OMe bond cleavage and the introduction of three molecules of dihydrogen, but occurring with net retention of all nine CO ligands.

Unfortunately, because of the low and highly variable product yields, only limited information could be obtained about the mechanism of the hydrogenation reaction. The reaction of (μ-D)Ru_3(μ_3-η^3-MeOCCPhCPh)$(CO)_9$ with H_2 gives (μ-H)$_3Ru_3$(μ_3-CCHPhCHDPh)$(CO)_9$ as the only alkylidyne product, showing that hydride migration occurred specifically to the 3-carbon of the allyl fragment. Bulky substituents of the 3-carbon of the dimetalloallyl fragment were shown to facilitate the hydrogenation. Furthermore, it was found that a relatively weak C–X bond for the 1-carbon is required. Hydrogenation of (μ-H)Ru_3(μ_3-η^3-EtSCCMeCMe)$(CO)_9$ was shown to give (μ-H)$_3Ru_3$(μ_3-CCHMeCH$_2$Me)$(CO)_9$ (15%) and $H_4Ru_4(CO)_{12}$. No alkylidyne, only $H_4Ru_4(CO)_{12}$, was isolated from the reaction of (μ-H)Ru_3(μ_3-η^3-Et$_2$NCCHCMe)$(CO)_9$ with dihydrogen. Pyrolysis of (μ-H)Ru_3(μ_3-η^3-MeOCCHCH)$(CO)_9$ in the absence of dihydrogen gave only intractable brown solids.

In the case of (μ-H)Ru_3(μ_3-η^3-EtSCCRCR)$(CO)_9$, the weakness of the C–S bond allows for facile isomerization to Ru_3(μ-SEt)(μ_3-η^3-CCRCHR)$(CO)_9$ in the absence of dihydrogen. This rearrangement incorporates two of the necessary steps in the hydrogenation of (μ-H)Ru_3(μ_3-η^3-EtSCCRCR)$(CO)_9$ to (μ-H)$_3Ru_3$(μ_3-CCHRCH$_2$R)$(CO)_9$—cleavage of the C–S bond and hydride migration to the 3-carbon of the "allyl" chain. Thus, the isomerization of (μ-H)Ru_3(μ_3-η^3-EtSCCMeCMe)$(CO)_9$ to Ru_3(μ-SEt)(μ_3-η^3-CCMeCHMe)$(CO)_9$ is probably the first step in the hydrogenation of (μ-H)Ru_3(μ_3-η^3-EtSCCMeCMe)$(CO)_9$ to (μ-H)$_3Ru_3$(μ_3-CCHMeCH$_2$Me)$(CO)_9$, and the analogous process presumably occurs during the hydrogenation of (μ-H)Ru_3(μ_3-η^3-MeOCCRCR)$(CO)_9$. Isomerization of (μ-H)Ru_3(μ_3-η^3-EtSCCRCR)$(CO)_9$ to Ru_3(μ-SEt)(μ_3-η^3-CCRCHR)$(CO)_9$ is favorable because of the relatively strong Ru–S bond and weak C–S bond; however, for (μ-H)Ru_3(μ_3-η^3-MeOCCRCR)$(CO)_9$ the much weaker Ru–O bond and stronger C–OMe bond prevent the thermal isomerization from occurring under conditions mild enough to allow isolation of the product.

At this time speculation concerning the mechanism of the isomerization is premature. The preliminary kinetic data are consistent with an intramolecular process. However, crossover experiments and kinetic isotope effect determinations will be necessary to establish the intramolecularity of the reaction and the importance of hydride migration in the rate-determining step. The crystal structure of Ru_3(μ-SEt)(μ_3-η^3-CCPhCHPh)$(CO)_9$ indicates that the hydride migation (or reductive elimination) occurs with retention of configuration at carbon, resulting in an anti relationship between the hydrogen and the substituent of the 2-carbon, information not provided by the isotope labeling in the product of hydrogenation of (μ-D)Ru_3(μ_3-η^3-MeOCCPhCPh)$(CO)_9$.

To demonstrate the intermediacy of the 1,1-dimetalloallyl isomer in the hydrogenation of (μ-H)Ru_3(μ_3-η^3-EtSCCMeCMe)$(CO)_9$ to (μ-H)$_3Ru_3$(μ_3-CCHMeCH$_2$Me)$(CO)_9$, we reacted Ru_3(μ-SEt)(μ_3-η^3-CCMeCHMe)$(CO)_9$ with dihydrogen under somewhat milder conditions (see Experimental Section) than were used previously for the hydrogenation of (μ-H)Ru_3(μ_3-η^3-EtSCCMeCMe)$(CO)_9$ (Figure 1, reaction ii). Indeed, (μ-H)$_3Ru_3$(μ_3-CCHMeCH$_2$Me)$(CO)_9$ was isolated, albeit in low yield, as required by the above proposal. The major product (μ-H)Ru_3(μ-SEt)$(CO)_{10}$ is a thermodynamic "sink" in this reaction because of the strong Ru–S bonds and is likely a product arising from cluster fragmentation. If (μ-H)Ru_3(μ-OMe)$(CO)_{10}$[17] were produced in the hydrogenation of (μ-H)Ru_3(μ_3-η^3-MeOCCRCR)$(CO)_9$, it would not be expected to survive the conditions required for hydrogenation.

Sulfur–carbon bond cleavage occurring on transition-metal centers is of interest as a model for heterogeneously catalyzed hydrodesulfurization[18] and also as a method of synthesizing larger metal clusters.[19] In only a few instances can the mechanism of the C–S bond cleavage and hydrogenation be easily studied. Because isomerization of (μ-H)Ru_3(μ_3-η^3-EtSCCRCR)$(CO)_9$ to Ru_3(μ-SEt)(μ_3-η^3-CCMeCHMe)$(CO)_9$ is essentially quantitative, and because a wide variety of substituted derivatives can be prepared, this system is useful in this context, and the mechanism is now under investigation. Unfortunately, the low yield of the hydrogenation reaction makes it very difficult to obtain further information concerning the mechanism of this second step. Different approaches through the syntheses and hydrogenations of more reactive analogues M_3(μ-X)(μ_3-η^3-CCRCHR)$(CO)_9$ differing in the nature of X (NR_2 or halide) and R (CMe_3 or CO_2Me) may provide still further information about this process.

Acknowledgment. The mass spectrometer (CHE-850962) and the Varian Gemini NMR spectrometer (CHE-8613066) used for this work were purchased with funds from the National Science Foundation. This work was supported by the National Science Foundation through Grant No. CHE-8520276 (J.B.K.) J.B.K. acknowledges the Alfred P. Sloan Foundation for support. We thank Mr. Leigh Nevinger for the mass spectral determinations.

Registry No. A (R = Ph), 100852-24-2; A (R = Me), 97633-76-6; B (R = Ph), 118377-64-3; B (R = Me), 100852-25-3; C, 97633-70-0; D, 23733-20-2; (μ-H)$_3Ru_3$(μ_3-CSEt)$(CO)_9$, 100852-22-0; C_2Ph_2, 501-65-5; C_2Me_2, 503-17-3.

Supplementary Material Available: Tables of anisotropic thermal parameters, C–C and C–H distances, and C–C–C(phenyl) angles and a stereoview of the molecule (3 pages); a listing of observed and calculated structure factor amplitudes (19 pages). Ordering information is given on any current masthead page.

(17) Aime, S.; Botta, M.; Gobetto, R.; Osella, D.; Padovan, F. *J. Chem. Soc., Dalton Trans.* **1987**, 253.
(18) Huckett, S. C.; Miller, L. L.; Jacobson, R. A.; Angelici, R. J. *Organometallics* **1988**, *6*, 686 and references therein.
(19) Adams, R. D. *Polyhedron* **1985**, *4*, 2003.